A COMPARISON BETWEEN IBM WITH FEEDBACK FORCING AND A VOLUME PENALIZATION METHOD FOR COMPRESSIBLE FLOWS ECCOMAS CONGRESS 2022

L. Ménez[1], E. Goncalves[1], P. Parnaudeau[1], D. Colombet [2]

[1] Pprime, UPR 3346 CNRS, ISAE-ENSMA
Université Poitiers 86961 Chasseneuil cedex, France
email: lucas.menez@ensma.fr

[2] LEGI, UMR 5519 CNRS
Université Grenoble Alpes 38400 St. Martin d'Hères, France

Key words: Immersed Boundary Methods, Penalization, Compressible flows

Abstract. The aim of this work is to model compressible flows involving shock waves past a solid obstacle using a non-conformal mesh. An Immersed Boundary Method (IBM) with feedback forcing and a volume penalization method are considered and compared. Both methods are validated on various test-cases. Accuracy and computational cost are discussed.

1 INTRODUCTION

In computational fluid dynamics, the body-fitted approach is classically adopted to model a fluid flow past a solid. Only the fluid domain is discretized, the mesh fits with the solid geometry and the boundary conditions are directly imposed at the interface between fluid and solid (Figure 1a). Other approaches are investigated in this work in order to use a non-conformal Cartesian mesh. In the IBM approach [1], the interface is discretized in addition to the Eulerian domain (Figure 1b). The boundary conditions at the interface between fluid and solid are imposed by computing and spreading a forcing term at the points of the discretized interface, denoted as Lagrangian points. In the Penalization method [2], the solid is considered as a porous medium and a forcing term is also added to the equations in order to model the solid obstacle (Figure 1c). No discretization of the interface is needed in this approach.

2 THEORETICAL FORMULATION

2.1 Navier-Stokes equations for compressible flows

Only two-dimensional flows are investigated in this study. To simulate such flows, the compressible Navier-Stokes equations are expressed as follows:

$$\dot{\boldsymbol{W}} + \boldsymbol{Q}(\boldsymbol{W}) + \boldsymbol{L}(\boldsymbol{W}) = \boldsymbol{f} \tag{1}$$

with $\boldsymbol{W} = (\rho, \rho u, \rho v, \rho E)^T$ the vector of conservative variables, $\boldsymbol{Q}$ the convective operator and $\boldsymbol{L}$ the diffusive operator. The system is closed by the perfect gas equation of state. The source term
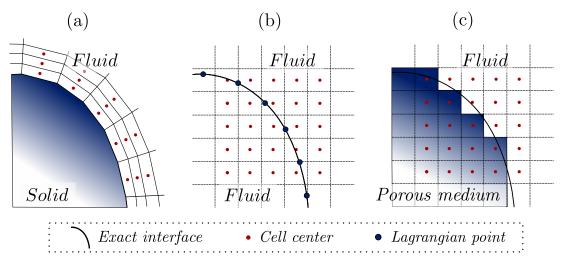
Figure 1: Few different approaches to model a solid in a fluid flow: (a) Body-fitted, (b) IBM, (c) Penalization

$\boldsymbol{f} = (f_\rho, f_u, f_v, f_E)^T$ models the presence of the solid. This forcing term is computed differently depending on the method that is adopted. With the two methods that are presented in the following sections, it is possible to impose a no-slip condition on the velocity at the fluid-solid interface and no specific treatment is applied on temperature in this work.

2.2 IBM with feedback forcing

Initially designed for incompressible flows [1] and then adapted to compressible flows [3], this method consists in calculating a forcing term at the fluid-solid interface, that is then spread at the vicinity of the interface. In addition to the Cartesian grid, it is necessary to discretize the Lagrangian contour representing the interface, as depicted in Figure 2a. The $\boldsymbol{X}$ points of the interface Γ are spaced by a Lagrangian discretization step Δs and the $\boldsymbol{x}$ points refer to the center of the Cartesian grid cells. The passage of quantities between the Eulerian and Lagrangian domains is performed by convolution with regularized Dirac functions, called δ functions [4][5][6].

The global approach of the method is first presented for the momentum equation. From the fluid velocity $\boldsymbol{u}(\boldsymbol{x}, t)$ on the Eulerian domain, the velocity at each point $\boldsymbol{X}$ of the interface is interpolated:

$$\boldsymbol{u}(\boldsymbol{X}, t) = \int_{D_{\boldsymbol{X}}} \boldsymbol{u}(\boldsymbol{x}, t) \delta_h(\boldsymbol{X} - \boldsymbol{x}) d\boldsymbol{x} \qquad (2)$$

with δ_h the δ function extended in 2D, $D_{\boldsymbol{X}}$ the support of δ_h centered in $\boldsymbol{X}$ and h the Eulerian discretization step. The forcing term is then computed at each Lagrangian point from (2):

$$\boldsymbol{F_u}(\boldsymbol{X}, t) = \alpha \int_0^t (\boldsymbol{u}_w - \boldsymbol{u}(\boldsymbol{X}, t')) dt' + \beta(\boldsymbol{u}_w - \boldsymbol{u}(\boldsymbol{X}, t)) \qquad (3)$$

with $\boldsymbol{u}_w$ the velocity imposed on the interface and (α, β) arbitrary parameters. The components of the source term on the momentum equation that appears in (1) are then computed by

spreading of (3) on the Eulerian domain:

$$\boldsymbol{f_u}(\boldsymbol{x}, t) = \rho(\boldsymbol{x}, t) \int_{D_{\boldsymbol{x}}} \boldsymbol{F_u}(\boldsymbol{X}, t) \delta_h(\boldsymbol{x} - \boldsymbol{X}) d\boldsymbol{X} \tag{4}$$

With a forcing term expressed as (3), the interpolated velocity $\boldsymbol{u}(\boldsymbol{X}, t)$ tends to the imposed velocity $\boldsymbol{u}_w$ as a harmonic oscillator with damping, with the angular frequency $\omega_0 = \sqrt{\alpha}$ and the damping coefficient $\xi = \beta/(2\sqrt{\alpha})$ depending on the arbitrary parameters α and β. The arbitrary parameters must be chosen in order to have a high damping coefficient in such a way that velocity converges quickly to the imposed one. The choice of these parameters leads to a stability condition on the time step depending on the chosen values.

No forcing is applied on the continuity equation ($f_\rho = 0$). About total energy, temperature is free at the interface and kinetic energy engendered by the momentum source term is added to the energy equation as a source term such that:

$$f_E(\boldsymbol{x}, t) = \boldsymbol{u}(\boldsymbol{x}, t).\boldsymbol{f_u}(\boldsymbol{x}, t) \tag{5}$$

By not imposing any forcing on the temperature, the fluid dynamics are similar to that of a flow past a solid with an adiabatic wall.
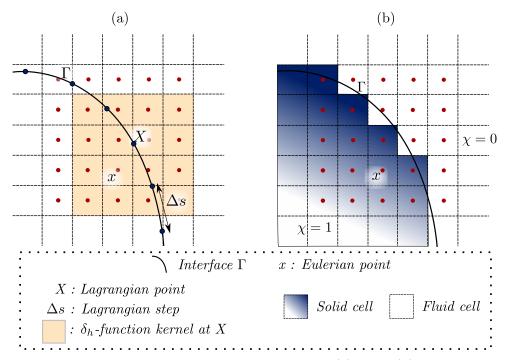

Figure 2: Illustration of the two present methods: (a) IBM, (b) Penalization

2.3 Volume penalization method

Contrary to the previous approach, the interface is not discretized in the penalization method [2]. The penalization term is directly computed on the Eulerian domain and is applied to the

whole solid, located with the mask function χ, that is equal to 1 in the solid and 0 elsewhere:

$$\chi(\boldsymbol{x}) = \begin{cases} 1 & \text{if } d(\boldsymbol{x}, \Gamma) \leqslant 0 \\ 0 & \text{otherwise} \end{cases} \tag{6}$$

with $d(\boldsymbol{x}, \Gamma)$ the signed distance between any point $\boldsymbol{x}$ and the interface Γ.

The principle of the method is to model the solid by a porous medium whose permeability tends to zero. In fact, the penalization term is inspired from the theory of compressible flows in porous media and is expressed as follows:

$$\boldsymbol{f}(\boldsymbol{W}) = \begin{pmatrix} -(\frac{1}{\phi} - 1)\chi\nabla.(\rho\boldsymbol{u}) \\ \frac{\chi}{\eta}(\rho u_w - \rho u) \\ \frac{\chi}{\eta}(\rho v_w - \rho v) \\ \frac{\chi}{\eta}(\boldsymbol{u}.(\rho\boldsymbol{u} - \rho\boldsymbol{u}_w)) \end{pmatrix} \tag{7}$$

with $\boldsymbol{u}_w = (u_w, v_w)^T$ the velocity condition imposed to the solid, ϕ the porosity parameter and η the permeability parameter. The term that is applied to the continuity equation has been introduced by Liu & Vasilyev [7] in order to better simulate the wave propagation in the context of an isothermal wall. In this study, only the contribution of the momentum forcing on the kinetic energy is embedded in the energy equation. It can be noted that in the fluid, the source term is null because $\chi = 0$ so the flow is not affected. The permeability parameter must tend to 0 in order to correctly model the imposed boundary conditions. In this work, the permeability parameter is set at $\eta = 10^{-10}$. The influence of the porosity parameter ϕ is investigated in the validation part.

3 Numerical resolution

The equation (1) is solved in the Finite Volume formalism. The convective flux is computed with an HLLC scheme and second order in space is reached using a MUSCL reconstruction [8][9]. The viscous flux is computed with a second-order centered scheme. The solution at instant t^n is first updated to an intermediate solution with the convective and viscous fluxes at first order in time. This intermediate solution is then updated to the solution at instant t^{n+1} by the source term with a first-order explicit Euler scheme in IBM and with a first-order semi-implicit Euler scheme in penalization due to the stiffness of the penalization term ($1/\eta \gg 1$). The Cartesian mesh is refined around the area of interest in which the space step is uniform, and then it is stretched with a hyperbolic progression to the edges of the domain (Figure 3). For supersonic flows, the whole vector of conservative variables $\boldsymbol{W}$ is imposed at the inlet and it is extrapolated at the outlet because all the characteristics are outgoing. In the case of a normal incident shock wave, non-reflection conditions are imposed at the inlet and outlet of the domain. In both cases, non-reflection conditions are applied at the top and bottom edges of the domain. At the interface between fluid and solid, a no-slip condition is imposed by the IBM or penalization. For all validation cases, the solid is centered at $(0, 0)$ in a rectangular domain.

4 Validation

Three validation test cases involving shock waves have been investigated in this study in order to validate the IBM with feedback forcing and the penalization method for different solid
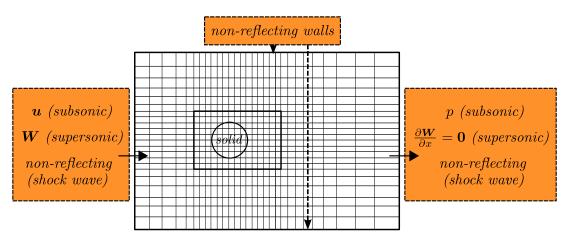
Figure 3: Mesh sketching and boundary conditions used in the present simulations

geometries. Both methods have been previously validated on steady and unsteady incompressible flows and are not presented in this work.

4.1 Case 1: Supersonic flow past a fixed cylinder $(M_\infty = 2, Re_D = 300)$

In this first case, a supersonic flow past a cylinder is considered. The Mach number is fixed at $M_\infty = 2$ and the Reynolds number at $Re_D = 300$, based on the far-field properties of the flow and the cylinder diameter D. Dimensions of the domain are $[-12.5D, 37.5D] \times [-15D, 15D]$. It is discretized in 430×351 cells, the minimum step size is set at $\Delta x_{min} = \Delta y_{min} = D/80$ and the CFL number is equal to 5.10^{-2} in IBM and 8.10^{-2} in penalization.

A bow shock appears upstream of the cylinder and the wake tends to become steady. The distance Δ_s between the shock front and the extremity of the cylinder along the stagnation line (Figure 4) can therefore be estimated. This distance, as well as the drag coefficient, are presented in Table 1 and show a relatively good agreement with the results of Riahi et al. [10] and Takahashi et al. [11].

$Ma = 2, Re = 300$	C_d	Δ_s
Takahashi et al. [11]	1.53	-
Riahi et al. [10]	1.51	0.69
IBM (present)	1.60	0.72
Penalization (present)	1.59	0.73

Table 1: Fixed cylinder at Mach 2: drag coefficient and distance of the shock front from the end of the cylinder

The pressure coefficient is also computed at the boundary of the cylinder. It can be achieved only after a pressure reconstruction at the interface because a non-conformal mesh is adopted in this work. The pressure coefficient represented in Figure 5a obtained with IBM fits with the results of Riahi et al. [10] while the one obtained with penalization fits with the results of Takahashi et al. [11]. Indeed, Riahi et al. also used a Lagrangian discretization while Takahashi
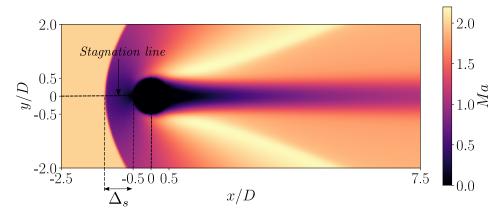
5

Figure 4: Fixed cylinder at Mach 2: Mach field and definition of the structure of the shock (the whole domain is not represented)

et al. adopted a ghost-cell method, in which the boundary conditions are imposed directly on the Eulerian cells. A body-fitted simulation has also been performed in order to compare the pressure profile along the stagnation line. It can be observed in Figure 5b that the pressure jump through the shock is well represented by both methods. The pressure obtained just after the shock and at the stagnation point are those expected by the Euler theory (p_2 and p_{i2}).

4.2 Case 2: Supersonic flow past a fixed triangle ($M_\infty = 2, Re_D = 50000$)

A supersonic flow past a fixed triangle is now investigated to study the behavior of both methods with wedges geometries. The Mach number is fixed at $M_\infty = 2$ and the Reynolds number at $Re_D = 50000$, based on the triangle length D. Dimensions of the domain are $[-1D, 3D] \times [-2D, 2D]$. It is discretized in 691×641 cells, the minimum step size is set at $\Delta x_{min} = \Delta y_{min} = D/250$ and the CFL number is equal to $4.7.10^{-2}$ in IBM and 0.19 in penalization.

The oblique shock is attached to the stagnation point, the flow is steady and the angle of the shock tends to a constant value denoted as β (Figure 6). The half-angle of the triangle is $\theta = 20°$.

| | Boiron et al. [12] | | Theoretical | IBM (present) | Penalization (present) | |
	Penalization	Body-fitted			$\phi = 1$	$\phi = 0.1$
C_d	0.74	0.71	0.68	0.58	0.66	0.67
β (°)	54.13	53.62	53.46	54.30	54.80	54.91

Table 2: Fixed triangle at Mach 2: drag coefficient C_d and shock angle β

Drag coefficient and shock angle obtained with both methods are compared with results of Boiron et al. [12] and theoretical results in Table 2. The value of the shock angle shows a well agreement for both methods but the drag coefficient is lower than expected for IBM. In fact, this method is not able to correctly model the downstream flow. It can be first observed with the pressure profile for $x/D \in [2, 3]$ in Figure 6. Then, the comparison of instantaneous
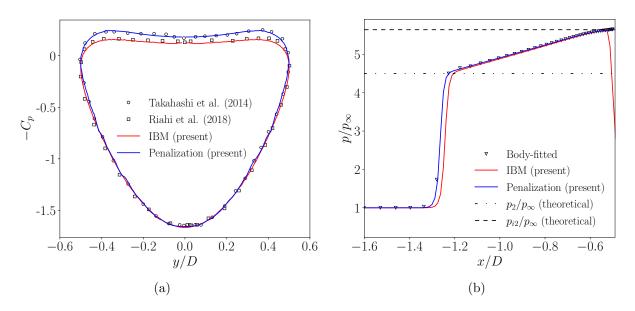
(a)

(b)

Figure 5: Fixed cylinder at Mach 2: (a) pressure coefficient, (b) pressure profile along the stagnation line
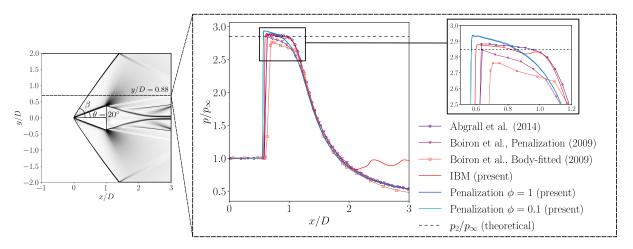

Figure 6: Fixed triangle at Mach 2: instantaneous Schlieren picture and pressure profile along the line $y/D = 0.88$

Schlieren pictures (Figures 7a and 7b) shows that the steady flow is not reached for IBM and that the downstream flow with the presence of a recirculation zone is not well modeled at all. It seems that the boundary conditions are not well imposed in critical areas with this approach, certainly due to the angulous corner. Furthermore, the pressure peak through the shock is well represented as shown in Figure 6. The porosity parameter ϕ that appears in the penalization term seems to have no influence on the shock position and on the pressure jump through the shock, when no specific treatment of temperature is applied at the fluid-solid interface.

In addition to the accuracy of numerical methods, computational cost also represents a major
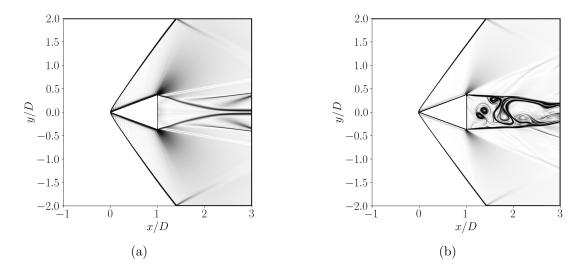
(a) (b)

Figure 7: Fixed triangle at Mach 2: instantaneous Schlieren picture obtained with (a) Penalization, (b) IBM

issue in a comparative study. Table 3 shows the computational time of IBM and penalization for the present test case. The difference between the two methods is incredibly high in terms of computational cost. In fact, penalization is 16.62 times faster than IBM. This is mostly due to the Lagrangian discretization in IBM that adds an extra dimension to the problem. An other reason of this gap is that the stiff forcing term is treated explicitly in IBM.

$\Delta x_{min} = 1/250$ (691 × 641) cells	IBM	Penalization	
		$\phi = 1$	$\phi = 0.1$
Comput. time (h)	161.56	9.72	40.00

Table 3: Fixed triangle at Mach 2: computational time for both methods (in hours)

4.3 Case 3: Shock/Cylinder interaction $(M_s = 2.81, Re_D = 3000)$

An interaction between an incident normal shock wave and a fixed cylinder is now investigated in order to study the behavior of both methods with unsteady shock waves. Dimensions of the domain are $[-3.75D, 11.25D] \times [-7.5D, 7.5D]$. It is discretized in 1340×1340 cells, the minimum step size is set at $\Delta x_{min} = \Delta y_{min} = D/160$ and the CFL number is equal to $4.8.10^{-2}$ in IBM and 0.19 in penalization. The normal shock wave is first generated by a discontinuous initialization in the domain. The left state and the right state are respectively:

$$\begin{pmatrix} P \\ \rho \\ u \end{pmatrix}_{\text{post-shock}} = \begin{pmatrix} 9.5.10^5 \text{ Pa} \\ 4.45 \text{ kg/m}^3 \\ 695.87 \text{ m/s} \end{pmatrix} ; \qquad \begin{pmatrix} P \\ \rho \\ u \end{pmatrix}_{\infty} = \begin{pmatrix} 10^5 \text{ Pa} \\ 1 \text{ kg/m}^3 \\ 0 \text{ m/s} \end{pmatrix} \qquad (8)$$

The normal shock wave moves from the left to the right at a Mach number equal to $M_s = 2.81$. Once that it reaches the cylinder position, the normal shock wave interacts with it. The final

8

time is set at $t_f = 3.10^{-7}$s, which corresponds approximately to the time taken by the incident shock wave to travel six cylinder diameters. A bow shock is formed upstream of the cylinder and the flow is composed by Mach stems, triple points, reflected shocks, slip-lines and vortices. The flow features are represented in Figure 8a. The triple points trajectories are plotted in Figure 8b for the upper part of the flow. They are compared with experimental and numerical results from literature. Results obtained with IBM and penalization show a good agreement with the reference results [13][14][15]. Similarly to the previous case, the influence of the porosity parameter ϕ has been investigated. It seems that ϕ has a weak influence on the wave propagation with this penalization model.

Table 4 shows the computational time that was needed to simulate the present case. The computations are 28.81 times faster with the penalization method ($\phi = 1$). It can also be observed that decreasing the porosity parameter ϕ increases the computational cost. In fact, the explicit treatment of the penalization term on the continuity equation has a significant impact on the time step.
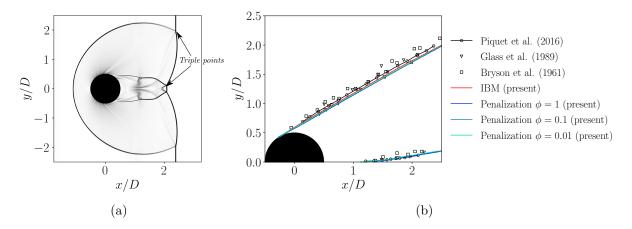

Figure 8: Shock/Cylinder interaction: (a) Instantaneous Schlieren picture, (b) Triple points trajectories

$\Delta x_{min} = D/160$ (1340 × 1340) cells	IBM	Penalization		
		$\phi = 1$	$\phi = 0.1$	$\phi = 0.01$
Comput. time (h)	142.60	4.95	5.57	36.80

Table 4: Shock/Cylinder interaction: computational time for both methods (in hours)

5   Conclusion

In this work, two methods to model a solid obstacle in a compressible flow involving shock waves have been adapted, validated and compared. These two methods make possible the use of a non-conformal mesh such as a Cartesian grid. Both methods showed a good agreement with the reference results, excepted IBM with wedge geometries. The forcing term being treated explicitly

in IBM, the arbitrary parameters α and β must be chosen carefully to ensure both accuracy and an acceptable time step. In fact, IBM is computationally expensive and the small time step is one of the reasons of this weakness. Another reason is that the Lagrangian discretization adds an extra dimension to the problem. The penalization method is less computationally expensive than IBM, as shown in Tables 3 and 4. This is due to the fact that the stiff penalization term is treated implicitly and that no interface discretization is needed with this approach. Although the interface between fluid and solid is not well represented, this method showed positive results for all geometries. It is also able to compute interface quantities correctly, such as pressure coefficient after a suitable reconstruction of these quantities at the interface.

6   Aknowledgments

REFERENCES

[1] C.S. Peskin. Flow patterns around heart valves: a numerical method. *Journal of Computational Physics*, 10(2):252–71, 1972.

[2] E. Arquis and J.P. Caltagirone. Sur les conditions hydrodynamiques au voisinage d'une interface milieu fluide-milieu poreux: Application à la convection naturelle. *Comptes Rendus de l'Académie des Sciences de Paris*, 299:1–4, 1984.

[3] Y.L. Qiu, C. Shu, J. Wu, Y. Sun, L.M. Yang, and T.Q. Guo. A boundary condition-enforced immersed boundary method for compressible viscous flows. *Computers & Fluids*, 136:104–113, 2016.

[4] R.P. Beyer and R.J. Leveque. Analysis of a one-dimensional model for the immersed boundary method. *Journal on Numerical Analysis*, 29:332–364, 1992.

[5] A.M. Roma, C.S. Peskin, and M.J. Berger. An adaptive version of the immersed boundary method. *Journal of Computational Physics*, 153:509–534, 1999.

[6] M.C. Lai and C.S. Peskin. An immersed boundary method with formal second-order accuracy and reduced numerical viscosity. *Journal of Computational Physics*, 160:705–719, 2000.

[7] Q. Liu and O.V. Vasilyev. A brinkman penalization method for compressible flows in complex geometries. *Journal of Computational Physics*, 227:946–966, 2007.

[8] E. Goncalves and P. Parnaudeau. Numerical study of pressure loads generated by a shock-induced bubble collapse. *Physics of Fluids*, 33, 2021.

[9] R. Dubois, E. Goncalves, and P. Parnaudeau. High performance computing of stiff bubble collapse on cpu-gpu heterogeneous platform. *Computers & Mathematics with Applications*, 99:246–256, 2021.

[10] H. Riahi, M. Meldi, J. Favier, E. Serre, and E. Goncalves. A pressure-corrected immersed boundary method for the numerical simulation of compressible flows. *Journal of Computational Physics*, 374:361–383, 2018.

[11] S. Takahashi, T. Nonomura, and K. Fukuda. A numerical scheme based on an immersed boundary method for compressible turbulent flows with shocks: Application to two-dimensional flows around cylinders. *Journal of Applied Mathematics*, ID 252478, 2014.

[12] O. Boiron, G. Chiavassa, and R. Donat. A high-resolution penalization method for large mach number flows in the presence of obstacles. *Computers & Fluids*, 38:703–714, 2009.

[13] A. Bryson and R. Gross. Diffraction of strong shocks by cones, cylinders, and spheres. *Journal of Fluid Mechanics*, 10(01):1–16, 1961.

[14] I. Glass, J. Kaca, and D. Zhang. Shock wave diffractions over semi-circular and half-diamond cylinders. *Twelfth Canadian congress of applied mechanics*, 1:596–7, 1989.

[15] A. Piquet, O. Roussel, and A. Hadjadj. A comparative study of brinkman penalization and direct-forcing immersed boundary methods for compressible viscous flows. *Computers & Fluids*, 136:272–284, 2016.